



# Interplay among Hydrogen Chemisorption, Intercalation and Bulk Diffusion at the Graphene Covered Ni(111) Crystal.

Monica Pozzo,<sup>†,‡</sup> Tommaso Turrini,<sup>¶</sup> Luca Bignardi,<sup>¶</sup> Paolo Lacovig,<sup>§</sup> Daniel  
Lizzit,<sup>§,△</sup> Ezequiel Tosi,<sup>§,▽</sup> Silvano Lizzit,<sup>§</sup> Alessandro Baraldi,<sup>¶,§</sup> Dario Alfè,<sup>||,⊥,#</sup>  
and Rosanna Larciprete\*,<sup>@</sup>

<sup>†</sup>*Department of Earth Sciences, Thomas Young Center, University College London, 5  
Gower Place London WC1E 6BS, U.K.*

<sup>‡</sup>*London Centre for Nanotechnology, University College London, 17-19 Gordon Street  
London WC1H 0AH, U.K.*

<sup>¶</sup>*Department of Physics, University of Trieste, Via Alfonso Valerio 2, 34127 Trieste, Italy*  
<sup>§</sup>*Elettra-Sincrotrone Trieste, S.S. 14 Km 163.5 in AREA Science Park, 34149 Basovizza,  
Trieste, Italy*

<sup>||</sup>*Department of Earth Sciences, Thomas Young Center, University College London, 5  
Gower Place London WC1E 6BS, UK*

<sup>⊥</sup>*London Centre for Nanotechnology, University College London, 17-19 Gordon Street  
London WC1H 0AH, UK*

<sup>#</sup>*Department of Physics "Ettore Pancini", Università Federico II, Via Cinthia 21, 80126  
Napoli, Italy*

<sup>@</sup>*CNR-Institute for Complex Systems, Via dei Taurini 19, 00133 Roma, Italy*

<sup>△</sup>*Current address: Polytechnic Department of Engineering and Architecture, University of  
Udine, 33100 Udine, Italy.*

<sup>▽</sup>*Current address: Instituto de Ciencia de Materiales de Madrid, (ICMM-CSIC), C/Sor  
Juana Inés de La Cruz 3, 28049 Madrid, Spain*

E-mail: [rosanna.larciprete@isc.cnr.it](mailto:rosanna.larciprete@isc.cnr.it)

## Abstract

The interaction between a Ni(111) substrate covered by a complete Gr monolayer and H atoms occurs through two parallel routes leading to the hydrogen chemisorption on graphene, and, at much lower rate but still with some ease, to the intercalation of H atoms below it. This latter reaction determines a direct interaction of the H atoms with the metal surface and eventually the H diffusion into the Ni bulk under the Gr cover. In this study we have combined high resolution X-ray photoelectron spectroscopy, thermal programmed desorption and density functional theory calculations to establish how the chemisorption and intercalation yields and their interplay depend on temperature and to find out how graphene affects the amount and the evolution of the hydrogen diffused in the Ni bulk. We found that, between 150 and 320 K, hydrogen chemisorption on Gr is independent of temperature and that Gr lifting, which signals the H intercalation below it, does not occur below 180-200 K, being limited by an energy barrier of the order of 150 meV. For the heavily hydrogenated samples, when H atoms diffuse also into the Ni bulk, the Gr cover plays a key role for H storage because it strongly enhances the amount of H loaded in the interface with respect to the bare Ni(111) substrate. This behavior, possibly exhibited also by other graphene/metal interfaces provided that intercalation of H below graphene can readily occur, might foster the design of innovative materials to be applied for H storage.

# Introduction

The worldwide interest in hydrogen production and storage is significantly renewing the attention toward the interaction of H atoms with metals,<sup>1-3</sup> with special focus on those particularly suited to bulk absorption. In this respect nickel, besides featuring a high catalytic activity, possesses a strong sorption ability which makes it elective materials for solid-state hydrogen storage systems, also in the form of Ni-based compounds and alloys. Therefore, the hydrogenation of nickel crystals, which has been extensively investigated throughout the 1990s and early 2000s,<sup>4-14</sup> is recently motivating new experimental and theoretical studies.<sup>15-19</sup> Concerning hydrogen loading in the Ni bulk, it is known that it requires the exposure to H<sub>2</sub> molecules at high pressure and high temperature, up to the formation of the metal hydride. Alternatively, hyperthermal H atoms, even at low temperatures, can penetrate the Ni surface and populate the Ni bulk. It has been shown that in this case the H atoms adsorb at subsurface sites, where are trapped by a shallow barrier, and from where they can re-emerge already at around 200 K. In order to maintain these atoms in the crystal up to higher temperatures, the capping effect provided by a high surface coverage might help, as the outdiffusion of bulk atoms is strongly limited if all available surface sites are occupied.<sup>7,15</sup> A mean for having the metal surface saturated with H, even above room temperature (RT), could be to cover the Ni crystal with a graphene layer, provided that hydrogen loading takes place by intercalation through it. The perspective that a graphene layer grown on the Ni surface might open new routes for hydrogen uptake with respect to the bare metal surface, together with the manifold of possible reactions which can occur between hydrogen and the Gr/Ni(111) interface,<sup>20-22</sup> makes this system worthy of deeper investigations. Recently we have shown that at RT the interaction of H atoms with the Gr/Ni(111) interface leads to rapid chemisorption on graphene, but also, with a slower rate to the intercalation below Gr.<sup>23</sup> In the latter process H atoms bind to the Ni surface where, because of the presence of graphene, they remain up to a few tens kelvin above RT. Moreover, thermal programmed desorption (TPD) measurements showed that the quantity of H stored below Gr exceeds



one monolayer, which is the saturation coverage for the Ni(111) surface hydrogenated by dissociative chemisorption of  $\text{H}_2$ , hinting at a contribution due to the release of H atoms diffused below the surface.<sup>23</sup> The possible enhancement of the hydrogen storage in the Ni bulk promoted by the presence of the Gr layer asks for a more detailed investigation. Moreover, the interplay between chemisorption and intercalation as a function of the temperature has to be carefully elucidated in order to understand how graphene impacts the different stages of the hydrogenation. Therefore, in this study we followed the hydrogenation of the Gr/Ni interface as a function of temperature by means of high resolution C1s core level spectroscopy combined with density functional theory (DFT) calculations. In some cases, besides monitoring the hydrogen uptake by means of surface spectroscopy, we measured by TPD the  $\text{H}_2$  released in the gas phase, which allowed the total amount of hydrogen loaded in the sample to be determined. The combined experimental and theoretical results provided invaluable contributions to the understanding of the complex manifold of surface and bulk reactions which regulate the interaction of H atoms with the Gr/Ni(111) interface. In the following, we first describe the effect of temperature on H chemisorption on Gr and intercalation below Gr, and finally illustrate the hydrogen diffusion in the Ni bulk and highlight the impact of Gr on the stability of the hydrogen-loaded interface.

## Materials and Methods

The experiment was performed at the SuperESCA beamline of the synchrotron radiation source Elettra (Trieste, Italy). A Ni(111) crystal was mounted on a manipulator capable of providing fast-rate sample heating and cooling. The sample was fixed to the cryostat by means of a Ta stick spot-welded on the back and was heated by W filaments placed behind. The thermocouples were spot-welded to the edge of the sample. Surface cleaning was performed by Ar ion sputtering at 1 keV followed by annealing up to 1000 K and finally checked by x-ray photoelectron spectroscopy (XPS) and low energy electron diffraction

(LEED). Graphene was grown on the Ni crystal held at 830 K by dosing ethylene, whose pressure was kept at  $1 \times 10^{-7}$  mbar and finally raised to  $5 \times 10^{-7}$  mbar. The growth was followed in real time by C1s spectroscopy. The complete coverage of the Ni substrate by graphene was achieved by prolonging the exposure to ethylene well beyond the saturation of the C1s peak intensity.

Hydrogenation was obtained by exposing the Gr/Ni(111) sample to the hydrogen flux, at a pressure, fixed for each experiment, in the range  $1 \div 5 \times 10^{-6}$  mbar. During exposure  $H_2$  was cracked by passing through a tungsten capillary heated by electron bombardment to 2800 K. The hydrogen cracker, which was partially shuttered to prevent the sample from being directly exposed to the flux of H atoms and to the radiation emitted by the hot cracker filament, was positioned close to the electron energy analyzer, with the tip at a distance of  $\sim 5$  cm from the sample. This geometry allowed to acquire sequences of fast XPS spectra during sample hydrogenation and during thermal desorption. Hydrogen atoms produced in the hot tube are estimated to have a kinetic energy of the order of  $\frac{3}{2}k_B T \sim 0.38$  eV. As for the cracking efficiency, we estimated that the fraction  $f$  of dissociated molecules at the sample surface was in the range  $0.7 \leq f \leq 0.9$ . Because of the uncertainty on the H/ $H_2$  ratio in the gas flux impinging on the sample, in the following we mention the total hydrogen dose  $d$ , as calculated from the pressure measured by the vacuum gauge, knowing that the atomic H is a fixed fraction  $f$  of it, because the cracker and the dosing conditions were kept stable during each experiment.

High resolution C1s spectra were measured at a photon energy of 400 eV, with a total energy resolution better than 50 meV. For each spectrum the binding energy was calibrated by measuring the Fermi level position of the Ni substrate. XPS measurements were performed with the photon beam impinging at grazing incidence ( $70^\circ$ ), while photoelectrons were collected at normal emission angle ( $0^\circ$ ). The C1s core level spectra were best fitted with Doniach-Šunjić functions convoluted with Gaussians, and a linear background. In the following, the hydrogen coverage on the Ni substrate  $\theta_{Ni}$  and the hydrogen coverage on

graphene  $\theta_{Gr}$  are given in monolayers, where  $1 \text{ ML}_{Ni} = 1.86 \times 10^{15} \text{ atoms/cm}^2$ , which is the atomic surface density of Ni(111). Because of the very small mismatch of about 1% between the Gr and Ni(111) lattice constants, in the Gr layer there are two C atoms per  $(1 \times 1)$  Ni unit cell, and therefore  $1 \text{ ML}_{Gr} = 2 \text{ ML}_{Ni}$ .

The TPD curves were recorded by a quadrupole mass spectrometer equipped with a quartz shield ('Feulner cup'<sup>24</sup>) with a sample-size opening. Before each measurement, the sample was placed in front of the cup, almost in contact with it, and was heated at a rate of 2 K/s. For the isothermal desorption measurements the Gr/Ni(111) surface was exposed each time to 30000 langmuir (1 langmuir =  $1.33 \times 10^{-6} \text{ mbar} \cdot \text{s}$ ) of hydrogen, a H dose sufficient to achieve extensive intercalation (see below) and thus nearly full decoupling of graphene from the Ni substrate. Then the sample was rapidly heated to the target temperature and the desorption was followed by C1s spectroscopy.

The calculations have been performed using spin polarised density functional theory (DFT) as implemented in the VASP code.<sup>25</sup> The systems were modeled with a slab with 5 layers of Ni in a 4x4 hexagonal supercell and a layer of 4x4 unit cell of graphene placed on top. The bottom three layers of Ni were kept frozen at their bulk geometry, with a lattice parameter of 2.492 Å. The rest of the system was fully relaxed using the rev-vdw-DF2 functional<sup>26</sup> until the largest residual force was less than 0.015 eV/Å. We employed the projector augmented method (PAW)<sup>27</sup> using PBE<sup>28</sup> potentials. The plane wave cutoff was set to 400 eV, and the relaxations were performed by sampling the Brillouin zone using 2x2x1 k-point grids. Energy barriers were calculated using the nudged elastic band method<sup>29</sup> using 7 images.

For the calculation we considered the Gr layer in the TOP-FCC configuration on Ni(111) and in the following indicate as  $C_{FCC}$  and  $C_{TOP}$  the graphene atoms staying at the *fcc* and *top* sites of the metal surface, respectively. The adsorption energy per hydrogen atom  $E_a^S$  on a bare substrate  $S$  (in this study  $S=\text{Ni, Gr}$ ) is defined by  $E_a^S = E(S + H) - E(S) - \frac{1}{2}E(H_2)$  where  $E(S + H)$  and  $E(S)$  are the total energies of the substrate plus a H adatom and of

the bare substrate, respectively, and  $E(H_2)$  is the total energy of a hydrogen molecule in the gas phase. With this definition, a more negative value of  $E_a^S$  corresponds to stronger binding of hydrogen to the surface.

## Results and Discussion

The role played by the substrate temperature in the H chemisorption on graphene and in the intercalation below it has been studied by exposing to the same hydrogen dose  $d=5$  klangmuir the sample held at temperatures  $T_d$  in the range 150-320 K. The C1s spectra measured for the sample hydrogenated at the different temperatures are shown in Figure 1a. More details of the hydrogenation at 220 and 300 K are illustrated in Figures 1b and 1c by the 2D intensity plots of the C1s spectra recorded during the exposure to the H flux. The figures also show the C1s spectra recorded at the two temperatures in correspondence of the saturated chemisorption on Gr (black curves) and at the end of the hydrogenation runs, the latter together with the best-fit curves and the spectral components. The assignments for all components, namely  $A_1$ ,  $A_2$ ,  $B_1$ ,  $B_2$  and  $C_1$ , are listed in the caption of Figure 1 and are based on the attributions derived by DFT calculations in Ref.,<sup>23</sup> whereas the complete data analysis can be found in the Supporting Information. In brief, hydrogen chemisorption on Gr results in C1s components due to C atoms directly involved in ( $A_1$  and  $A_2$ ) or first neighbors of ( $B_1$  and  $B_2$ ) C-H bonds, whereas intercalation below Gr determines the appearance of the component  $C_1$ , which arises from the Gr regions decoupled from the substrate by the H atoms bonded to the Ni(111) surface. From now on, for the sake of simplicity, we will take into account only  $A_1$  to monitor the H chemisorption on Gr and will follow  $C_1$  to track the H intercalation below Gr.

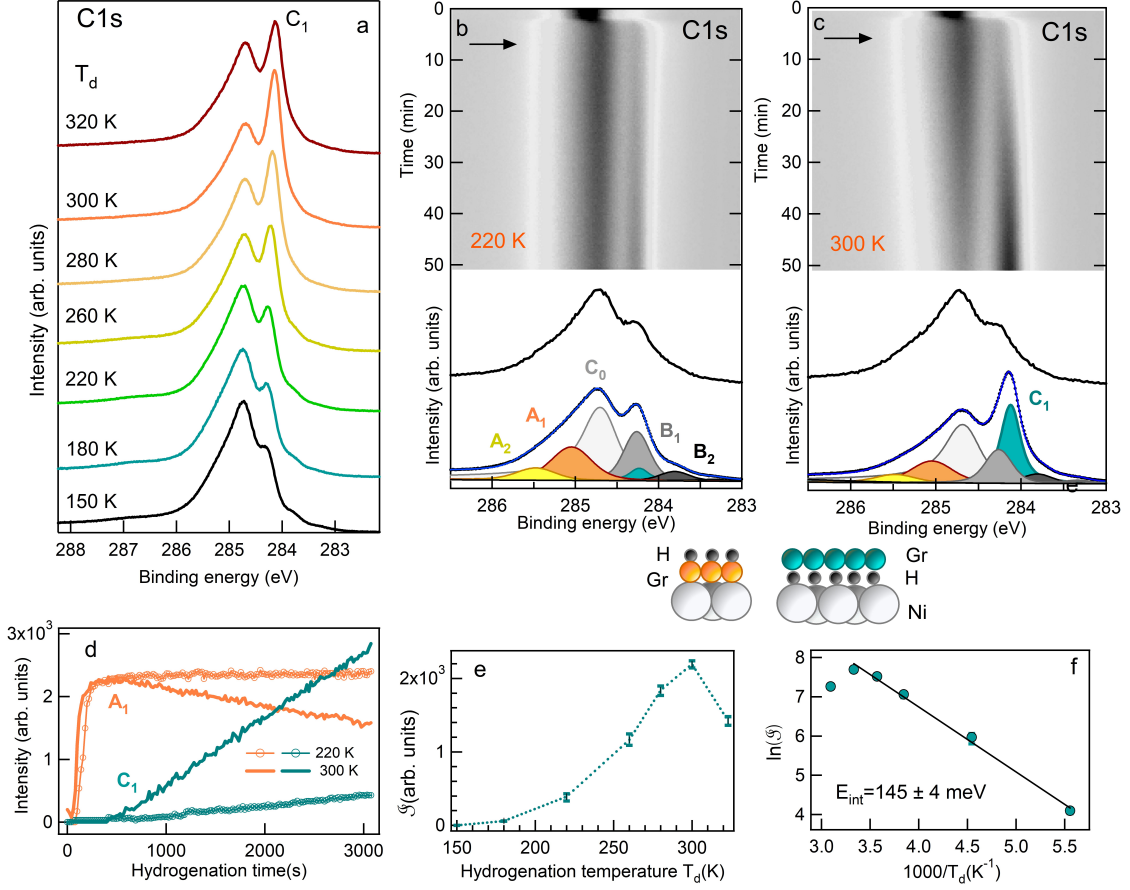


Figure 1: **Hydrogenation of Gr/Ni(111) as a function of temperature** (a) High resolution C1s spectra measured on the Gr/Ni(111) surface hydrogenated at different temperatures. (b-c) 2D plots of the C1s spectra measured during the exposure of the sample to 5 klangmuir of hydrogen at 220 and 300 K. The middle and the bottom curves show in each case the C1s spectra measured (middle curve) at the saturation of the chemisorption phase in correspondence of the arrows in the top panels and (bottom curves) at the end of the hydrogenation runs. In the latter case the best-fit curves and the spectral components obtained by following Ref.<sup>23</sup> are also shown. Unhydrogenated C atoms (dark gray atoms) are represented by  $C_0$  (284.68 eV); according to the calculations reported in Ref.<sup>23</sup> C atoms directly bonded to H contribute to  $A_2$  (285.44 eV) (H monomers and dimers) and to  $A_1$  (285.05 eV) (dimers, but mainly H trimers or larger clusters); graphene sites first neighbors of the C–H bonds result in  $B_1$  (284.28 eV) (neighbors of one and two C–H bonds) and  $B_2$  (283.84 eV) (neighbors of three C–H bonds); the  $C_1$  peak (284.15 eV) arises from the Gr regions decoupled from the Ni substrate (blue atoms) by the intercalated H atoms bonded to the substrate. (d) Integrated intensity of the  $A_1$  and  $C_1$  components, as a function of the hydrogenation time at 220 and 300 K. (e) Integrated intensity  $\mathcal{J}$  of the  $C_1$  component plotted as a function of the hydrogenation temperature  $T_d$ . (f) Arrhenius plot of  $\ln(\mathcal{J})$  vs.  $1/T_d$ .

## Chemisorption

As reported in Ref.,<sup>23</sup> the hydrogenation of the Gr/Ni(111) surface at RT initiates with the chemisorption on Gr of isolated H monomers and dimers followed by the formation of larger clusters. This process is optimally monitored by the C1s component  $A_1$ , whose intensity, measured as a function of time during the hydrogenation at 220 and 300 K is plotted in Figure 1d.

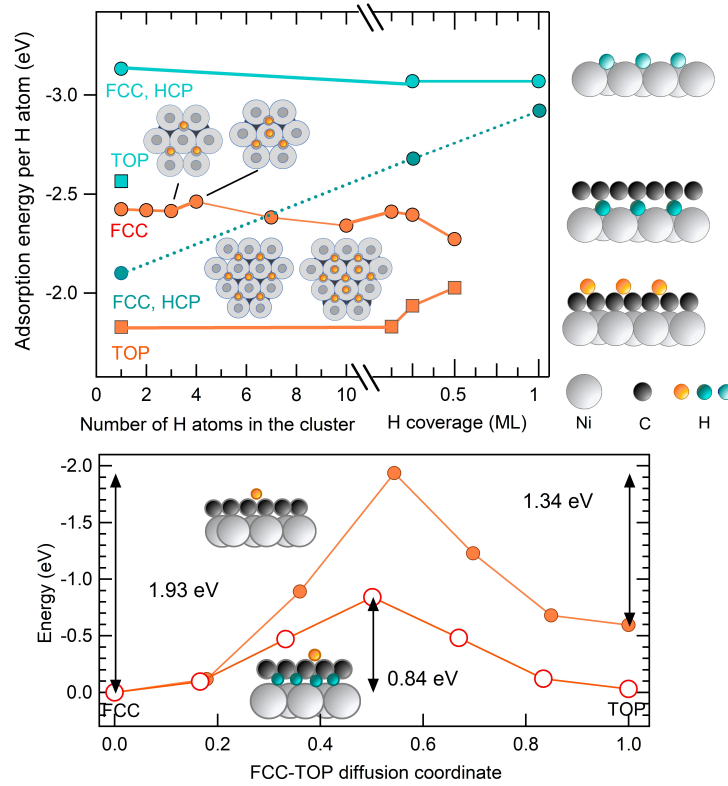


Figure 2: **Energetics of the hydrogenated Gr/Ni(111) interface.** (*top*) Adsorption energies calculated for H atoms chemisorbed as monomers, clusters (see schemes in the figure) or ordered superstructures on  $C_{FCC}$  and  $C_{TOP}$  graphene atoms (orange curves), on the bare Ni(111) surface (light green curve), and on Ni(111) surface covered by the Gr layer (dark green curve), as sketched on the side. (*bottom*) Diffusion energy barrier for a H atom moving from the  $C_{FCC}$  to the  $C_{TOP}$  site on Gr covering the Ni(111) surface (filled orange dots) and detached from the Ni(111) surface by 1  $ML_{Ni}$  of intercalated H chemisorbed in the  $Ni_{HCP}$  sites (empty orange dots).

The curves show that, in our hydrogenation conditions, chemisorption proceeds very fast and saturates within 10-50 s, with the  $A_1$  peak reaching the same intensity at the two

temperatures, which corresponds to the coverage of  $0.20 \div 0.25 \text{ ML}_{GR}$ . The C1s spectra measured in correspondence of the saturated chemisorption in the two cases are shown as black curves in the middle of Figures 1b and 1c. The close similarity between these two and any other C1s spectrum measured in this experiment just after the saturation of the chemisorption phase indicates that, at least in the investigated thermal range, the maximal amount of H bonded to Gr is independent from the substrate temperature.

Possible mechanisms which can impede the achievements of coverages higher than  $\sim 0.25 \text{ ML}$ , can include the decay of the chemisorption cross section with increasing cluster size and/or the occurrence of reactions competing with chemisorption. In order to evaluate the first possibility we have calculated the adsorption energy  $E_a^{GR}$  of H atoms in different configurations on the Gr/Ni(111) surface (see Figure 2). In agreement with the results reported in the literature<sup>20,21,23,30</sup> we found that for isolated H atoms it is significantly more convenient to bind in top configuration to  $C_{FCC}$  graphene atoms ( $E_a^{GR} = -2.42 \text{ eV}$ ), than to  $C_{TOP}$  atoms ( $E_a^{GR} = -1.83 \text{ eV}$ ). When going to H dimers, trimers and eptamers in  $C_{FCC}$  sites, the adsorption energy per atom varies only negligibly ( $|\Delta E_a^{GR}| < 0.1 \text{ eV}$ ) even if the intermediate  $C_{TOP}$  sites are hydrogenated (tetramer and decamer, see Figure 2). Ordered superstructures corresponding to coverages  $\theta_{GR}$  between 0.125 and  $0.5 \text{ ML}_{GR}$  show a slight tendency to lower (higher) stability with increasing  $\theta_{GR}$  when bonded to  $C_{FCC}$  ( $C_{TOP}$ ) sites, so that the difference in the adsorption energy per H atoms between having all  $C_{FCC}$  sites ( $E_a^{GR} = -2.27 \text{ eV}$ ) or all  $C_{TOP}$  sites ( $E_a^{GR} = -2.03 \text{ eV}$ ) hydrogenated is only  $-0.24 \text{ eV}$ . Then small H assemblies are slightly favored with respect to large clusters or extended superstructures. Such an energy gain, although quite limited, might drive the chemisorption promoting sparse rather than heavily clustered configurations. However, for any of the explored temperatures it can be excluded that surface diffusion might play a role in stabilizing the H configurations toward those energetically more favorable. As can be seen in Figure 2b, the calculated diffusion barriers for a H monomer from the  $C_{FCC}$  to the  $C_{TOP}$  site and vice versa are  $1.93$  and  $1.34 \text{ eV}$ , respectively. These values are in close agreement with those calculated by

Zhao et al.,<sup>20</sup> who have also reported that for the transition from ortho-dimers or para-dimers towards meta dimers, the barriers are  $\sim 1.4$  eV and become higher for the inverse paths. Such physical constraints immobilize the chemisorbed H atoms in their residence sites preventing any diffusion at the investigated temperatures.

When considering whether chemisorption is limited by competing desorption processes, Langmuir-Hinshelwood (LH), Eley-Rideal (ER) and hot atom (HA) reactions have to be considered. The first mechanism, which consists in the recombination of two chemisorbed H diffusing close to each other and forming a desorbing  $H_2$  molecule, is hindered by the high barriers for surface diffusion, which cannot be overcome at the temperatures of our experiments. ER and HA desorption require that an energetic atom impinging from the gas phase ends up close enough to a chemisorbed H and consumes its residual kinetic energy for the desorption of a  $H_2$  molecule. In the ER reaction the incoming atom recombines directly with an adsorbate in a single collision event, whereas in the HA reaction, the projectile impacts several times with the surface before recombination.<sup>31</sup> In both cases, the probability that an impinging atom finds the chemisorbed H on its path depends on the surface coverage. Therefore, desorption is reasonably negligible at low coverage, whereas at moderate coverage becomes competitive with chemisorption. It is worth considering that if the excess energy of the impacting H atoms was predominantly dissipated through the excitation of the lattice motion, the energy available for molecular desorption would be reduced and the chemisorption yield enhanced with decreasing temperature. The stable chemisorption efficiency revealed by the maximal intensity of the  $A_1$  component in the C1s spectra, which is similar at all investigated temperatures (see Figure 1d), indicates that the relaxation to the substrate is not the dominant channel, in agreement with the fact that it occurs on a time scale much slower than the surface drift.<sup>32,33</sup> Then, it turns out that the factors limiting the coverage for the chemisorption of H atoms on the Gr/Ni(111) surface are the weak dependence of the adsorption energy on the cluster size and the occurrence of the desorption reactions triggered by the incoming H flux.



## Intercalation

Prolonged exposure to H atoms leads to intercalation below Gr. The penetration of H below graphene is revealed in the C1s spectrum by the appearance of the narrow C<sub>1</sub> peak around 284.1 eV (see Figure 1), which arises from the Gr regions where the interaction with the Ni substrate has been relieved.<sup>34,35</sup> Even after heavy hydrogen doses corresponding to complete lifting of the graphene layer, we found that the integrated area of the C1s spectra was stable within the error bar of 2% (see Figure SI3), indicating that, at the conditions adopted in our experiments, the Gr coverage can be considered stable during hydrogenation. The integrated intensity  $\mathfrak{I}$  of peak C<sub>1</sub> measured on the hydrogenated sample, which is plotted vs the dosing temperature in Figure 1e, shows that intercalation becomes clearly evident only starting from  $T_d=220$  K and that the amount of H that intercalates below Gr increases with  $T_d$  and reaches a maximum around 300 K. Above this temperature the desorption of the intercalated H atoms intervenes.<sup>23</sup> The Arrhenius plot of  $\ln(\mathfrak{I})$  vs.  $1/T_d$  (see Figure 1f) indicates that the activation energy  $E_{int}$ , which regulates the C<sub>1</sub> intensity, is of the order of 150 meV.

The origin of this barrier can be related to several factors. Usually intercalation is believed to occur through lattice defects. On the other hand, recently it has been observed experimentally<sup>36</sup> and explained theoretically<sup>37</sup> that H atoms adsorbed on defect-free Gr can flip on the other side with an activation energy of about 1 eV. In the thermal range explored here, overcoming this barrier would be quite improbable for chemisorbed H atoms, although, from the mere point of view of energetics, passing through graphene would be accessible to the hyperthermal H atoms impacting on it. However, in the case of complete graphene monolayers, other Gr/metal systems such as Gr/Ir(111), after having been extensively hydrogenated by means of a flux of H atoms, still appear impermeable to hydrogen, as no signs of intercalations are detected.<sup>38</sup> Therefore, we might consider the penetration of intact Gr as a possible, although minor, reaction route and consider much more likely the mechanism of H intercalation through surface defects. Then, the main requirement necessary for extensive intercalation to occur is a reasonable surface mobility of the H atoms both on Gr and on

the Ni substrate. As discussed above, at the investigated temperatures, H chemisorbed on Gr/Ni(111) can be taken as immobile. However, as shown in Figure 2b the energy barrier for H diffusion on graphene is almost halved (0.84 eV) if a monolayer of H is chemisorbed on the Ni surface. This means that the possibility of moving around for the H atoms chemisorbed on Gr increases in concert with intercalation. Instead, at low intercalated H coverage, the main route leading to intercalation remains the impact of the impinging HA in direct correspondence or in proximity of defect sites (monovacancies, divacancies, Stone-Wales defects and domain boundaries) in the graphene lattice, which are then reached by drifting on the surface.<sup>31</sup> In this respect, hot atoms, that is atoms with energies larger than the thermal energies of substrate atoms, can travel over long distances,<sup>32</sup> between tens and hundreds of angstrom.<sup>33</sup> For the H atoms which have approached the defects, the next step is the penetration below graphene. At this point, the other obstacle that the intercalated atoms have to overcome is the diffusion on the Ni surface away from the Gr defect sites, a process needed to leave the path free for other intercalants. The energy barrier for H diffusion on the Ni(111) surface has been determined to be 150-200 meV<sup>5,39</sup> for the bare metal and 200 meV on the Ni(111) surface under the graphene cover,<sup>39</sup> which is not far from the experimental value of 145 meV we found for  $E_{int}$ . Then, we are led to the conclusion that the factor limiting the rise of the C<sub>1</sub> peak intensity, and therefore the rate of intercalation below graphene, is the H diffusion barrier on the Ni(111) surface.

## Chemisorption vs. Intercalation

For the incoming hyperthermal H atoms drifting on Gr, the destiny is determined by the energetic balance between two possibilities, i.e. staying on graphene or passing through the defects and moving to the Ni surface. We calculated that for a single H atom intercalated below Gr, the chemisorption energies at the *hcp*, *fcc* or *bridge* sites of the Ni(111) surface are nearly equivalent, ( $E_a^{Ni} = -2.10 \div -2.12$  eV), whereas the *top* site is unfavorable ( $E_a^{Ni} = -0.95$  eV). Then, a H monomer is more stable when chemisorbed on Gr ( $E_a^{GR} = -2.42$  eV) than on

Ni underneath. However, as shown in Figure 2a, the H chemisorption energy on Ni below Gr decreases with increasing intercalated coverage ( $E_a^{Ni} = -2.70$  eV at  $0.25 \text{ ML}_{Ni}$  and  $-2.94$  at  $1 \text{ ML}_{Ni}$ ), which means that the presence of H on the Ni surface favors further intercalation. The Ni-H bonds, however, are not stabilized by Gr, as the calculated adsorption energy at both the *fcc* and *hcp* sites of the bare Ni(111) ( $E_a^{Ni} \sim -3.1$  eV) is much lower regardless of the coverage (see Figure 2a). In this respect we found that the increase  $\Delta E_a^{Ni}$  of adsorption energy on the Ni surface due to the presence of graphene overlayer is  $\sim 1$  eV for a single H adatom and diminishes to 0.3 and 0.1 eV when the coverage reaches 0.25 and 1  $\text{ML}_{Ni}$ , respectively. These values are in close agreement with Zhou *et al.*<sup>39</sup> who attributed the increase ( $\Delta E_a^{Ni}=0.23$  eV at  $0.25 \text{ ML}_{Ni}$ ) to the energy penalty paid to lift graphene and to a partial repulsion of the H and Ni electron clouds caused by the lower H-Ni distance.

The comparison between the  $A_1$  and  $C_1$  components of the C1s spectrum plotted in Figure 1d vs. the H dosing time allows the chemisorption and intercalation yields to be evaluated. It turns out that  $A_1$  at 220 K remains constant at the value reached after the saturation of chemisorption, whereas at 300 K it decreases in concert with the rise of  $C_1$ . In fact, complete lifting of Gr corresponds to a nearly H-free graphene surface, as it can be observed in the STM images<sup>23</sup> showing, in the heavily hydrogenated regions, the honeycomb lattice of the clean surface. At a first glance this behavior could be rationalized by considering that the role played by the C-Ni bonds in balancing the formation of the C-H bonds,<sup>20</sup> in the presence of intercalated H is somehow weakened. Conversely, this hypothesis is disclaimed by the DFT calculations, which indicate that large H clusters on Gr remain unaffected by the presence of 1  $\text{ML}_{Ni}$  of intercalated H (see Table 1), whereas the isolated H monomer, whose  $E_a^{GR}$  decreases from -2.42 to -2.83 eV, even benefits from the large H coverage underneath. Then, the vanishing H coverage on Gr can be likely attributed to a higher chemisorption barrier and/or to a higher ER desorption cross section in the Gr regions decoupled from Ni. If so, under the flux of H atoms, H desorption tends not to be balanced by new chemisorption and the net result is the ultimate depopulation of graphene.

## Diffusion in the Bulk

Once intercalation has set in, the way hydrogen settles at the Gr/Ni interface determines the possibility to implement this system for energy storage.

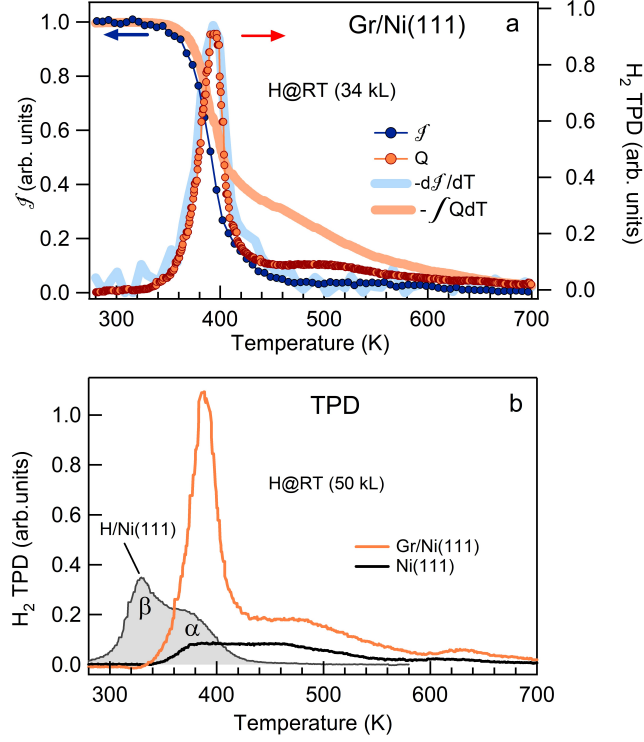


Figure 3: **Hydrogen release from Gr/Ni(111) and bare Ni(111)** (a) Comparison between the integrated intensity  $\mathfrak{J}$  of the  $C_1$  peak and the TPD signal  $Q$  measured during the thermal annealing of the Gr/Ni(111) sample dosed with 34 klangmuir of hydrogen at room temperature. The curves representing  $-d\mathfrak{J}/dT$  and  $-\int QdT$ , normalized to the maxima of  $Q$  and  $\mathfrak{J}$ , respectively, are also shown. (b) TPD curves measured while heating the Gr/Ni(111) (orange curve) and the bare Ni(111) (black curve) samples exposed to 50 klangmuir of hydrogen at room temperature. The solid gray curve is the TPD signal measured for the Ni(111) surface hydrogenated at saturation with  $H_2$  molecules at 150 K.

Valuable information is obtained by following the evolution with the temperature of the H loaded in the sample. This is shown in Figure 3a for the Gr/Ni(111) sample dosed with 34 klangmuir of hydrogen. The figure compares the desorption of the H coverage on the Ni surface  $\theta_{Ni}$ , traced by the decay of the integrated intensity  $\mathfrak{J}$  of the peak  $C_1$  (dotted black curve), with the total amount of released  $H_2$ , monitored by the TPD curve (red dotted curve). It turns out that  $\mathfrak{J}$  drops abruptly around 390 K and disappears. By contrast, the

TPD signal  $Q$ , in addition to the sharp desorption peak at  $\sim 394$  K which mirrors the fast  $\mathfrak{I}$  decay, shows also a broad shoulder extending up to 550 K. If  $\text{H}_2$  desorption originated exclusively from surface adatoms, then  $Q \propto -d\theta_{\text{Ni}}/dT \propto -d\mathfrak{I}/dT$ . The last term, plotted in Figure 3a (light blue curve), precisely reproduces the sharp TPD peak, but does not trace the broad shoulder, which, evidently, does not arise from H atoms staying at the Ni surface, but has a different origin. Analogously,  $-\int Q dT$  (pink curve), well reproduces the abrupt decay of  $\mathfrak{I}$  around 360 K, but then shows a long tail, counter part of the broad shoulder in the  $Q$  signal. As we demonstrate below, the  $\text{H}_2$  desorption delayed with respect to the sharp peak likely originates from H atoms diffused in the bulk of the Ni substrate. The sharp TPD peak corresponds approximately to the desorption of  $1.6 \text{ ML}_{\text{Ni}}$  over the total amount of  $2.2 \text{ ML}_{\text{Ni}}$  released in the whole thermal range. More importantly, such amount significantly exceeds the saturation coverage  $\theta_{\text{Ni}}=1 \text{ ML}_{\text{Ni}}$ , which is reached by low temperature dissociative chemisorption of  $\text{H}_2$ .<sup>4</sup> Larger  $\theta_{\text{Ni}}$  values are in principle possible when dosing H atoms, and in this respect we find that for the Ni(111) surface where all *fcc* and *hcp* sites are hydrogenated ( $\theta_{\text{Ni}} = 2 \text{ ML}_{\text{Ni}}$ ), the adsorption energy per H atom is -2.29 eV. However, for the bare Ni(111) exposed to the H atom flux, experimental results<sup>6,10,12</sup> and DFT calculations<sup>15,17,40,41</sup> indicate that, at high surface coverage, H atoms tend to penetrate subsurface, where they are kinetically trapped at metastable octahedral and tetrahedral sites. Moreover, subsurface H atoms can also easily diffuse deeper in the bulk. By assuming that a similar trend holds also under the graphene cover, it seems reasonable to relate the amount of H in excess with respect to  $1 \text{ ML}_{\text{Ni}}$  revealed by TPD, to a contribution from the bulk hydrogen, rather than to the extra-hydrogenated Ni surface.

Concerning the stability of the subsurface H atoms, for the Ni(111) surface dosed at low temperature it has been demonstrated that they resurface with several tenths of electronvolt excess energy,<sup>7,9,11</sup> recombine with surface atoms and desorb between 180 and 215 K as  $\text{H}_2$ .<sup>10,42</sup> These experimental results have motivated many theoretical studies,<sup>7-9,11,15,17,40,41,43</sup> which found that the heights of the diffusion barriers from subsurface to surface sites depend

on lattice relaxation, surface and subsurface H coverages and also, at low temperature, tunneling effects and correlated motion of the hydrogen and nickel atoms. Anyhow, there is a general agreement on the fact that a high occupation number of surface sites decreases the resurfacing rate. Shirazi et al.<sup>15</sup> calculated that the energy barrier for resurfacing increases from 0.05 to 1 eV, with  $\theta_{Ni}$  rising from 0.5 to 1.5  $ML_{Ni}$ , whereas Baer et al.<sup>7</sup> found that when a surface atom in the 3-fold hollow site blocks the exit of a subsurface hydrogen atom, the resurfacing barrier is raised to 1.2 eV. On the contrary, at surface coverage well below 1  $ML_{Ni}$  the bulk H are stable only at low temperatures. For a bare metal exposed to the H flux, the occurrence of ER and HA desorption reactions tend to lower the surface coverage. Moreover, in any case surface adatoms unavoidably start to desorb from Ni(111) around 300 K<sup>4</sup> (see Figure 3b), which means that the subsurface states are significantly populated only if continuously refilled by the H flux in a dynamical equilibrium. Therefore, a mean to rise the stability of subsurface H is to increase  $\theta_{Ni}$ , and in this respect the graphene cover can play an important role, as, at least, it effectively shields the incoming H flux.

In order to establish whether the graphene layer really enhances the H storage efficiency, we exposed at RT the bare and the Gr-covered Ni(111) surface to the same dose of H atoms (50 klangmuir), by adopting the same H exposure parameters (flux, exposure time and geometry) and measured by TPD the amount of H<sub>2</sub> released in the two cases. The results are shown in Figure 3b. The amount of H<sub>2</sub> released by Ni(111) and Gr/Ni(111) is 0.6 and 2.9  $ML_{Ni}$ , respectively. With respect to the TPD curve measured for the Ni(111) hydrogenated at saturation by low temperature dissociation of H<sub>2</sub> (filled gray curve in Figure 3b), where the presence of both  $\alpha$  and  $\beta$  peaks corresponds to  $\theta_{Ni} = 1 ML_{Ni}$ ,<sup>4</sup> in the TPD curve measured for the Ni(111) dosed at RT with H atoms, the  $\beta$  peak is absent because the corresponding state does not get populated at RT,<sup>44</sup> and the intensity of the  $\alpha$  peak is strongly reduced. Such a low coverage has to be related to the low sticking coefficient at 300 K (at least at kinetic energy<sup>45</sup> and geometry used in this experiment) and to the balance between chemisorption and desorption (HA and ER reactions) rates, which

might largely favor H removal.<sup>10</sup> Moreover it is also possible that some of the loaded H has desorbed during the permanence in UHV after the switching-off of the H flux.<sup>46</sup> Instead, for Gr/Ni(111) most of the H<sub>2</sub> is released in the sharp peak at 395 K. For both samples, the surface desorption is indiscernible from the broad TPD shoulder, which extends beyond 500 K, and that reasonably mirrors the time required by the deeply diffused atoms to resurface during the thermal ramp,<sup>47,48</sup> because prolonged exposure time at RT enhances H transport away from the surface.<sup>49</sup> The weak peak appearing at 630 K in the TPD curve of the Gr covered sample is due to the desorption of a tiny quantity of residual H atoms chemisorbed on Gr.<sup>23</sup>

Actually, for Gr/Ni(111), the large amount of H<sub>2</sub> released demonstrates that the presence of Gr allows hydrogen to accumulate at the interface and the abrupt desorption indicates that the energetic constraints, which stabilize the adsorbed and absorbed hydrogen, are suddenly released. In this respect it is worth noting that, because most of the hydrogen loaded in the Gr/Ni(111) interface is released a few tens kelvin above RT, the impact that the graphene coating would have on the retrieve of the stored fuel appears quite modest. Interestingly, subsurface H atoms have been observed also after the low-temperature hydrogenation of other metals like Pd<sup>50</sup> and Cu,<sup>51</sup> which, as nickel crystals, allow the epitaxial growth of Gr monolayers. Then, it would be undoubtedly worth finding out whether, also in these cases, the bulk absorption of hydrogen would benefit, in terms of thermal stability, from the presence of a complete Gr layer coating the metal substrate, provided that the conditions for efficient H intercalation below Gr are encountered. In order to explain the enhanced bulk absorption with respect to the bare surface, we considered the possibility that Gr had the capability to stabilize the subsurface sites with respect to the bare Ni surface, by calculating the adsorption energies in the octahedral and tetrahedral subsurface sites under the fully hydrogenated Ni(111) surface ( $\theta_{Ni}=1$  ML) with and without graphene. We found that the presence of Gr does not change the binding energies of isolated H atoms ( $E_a^{Ni}=-2.9$  eV), or even of a full H monolayer ( $E_a^{Ni}=-2.7$  eV), absorbed in the subsurface sites, which remain

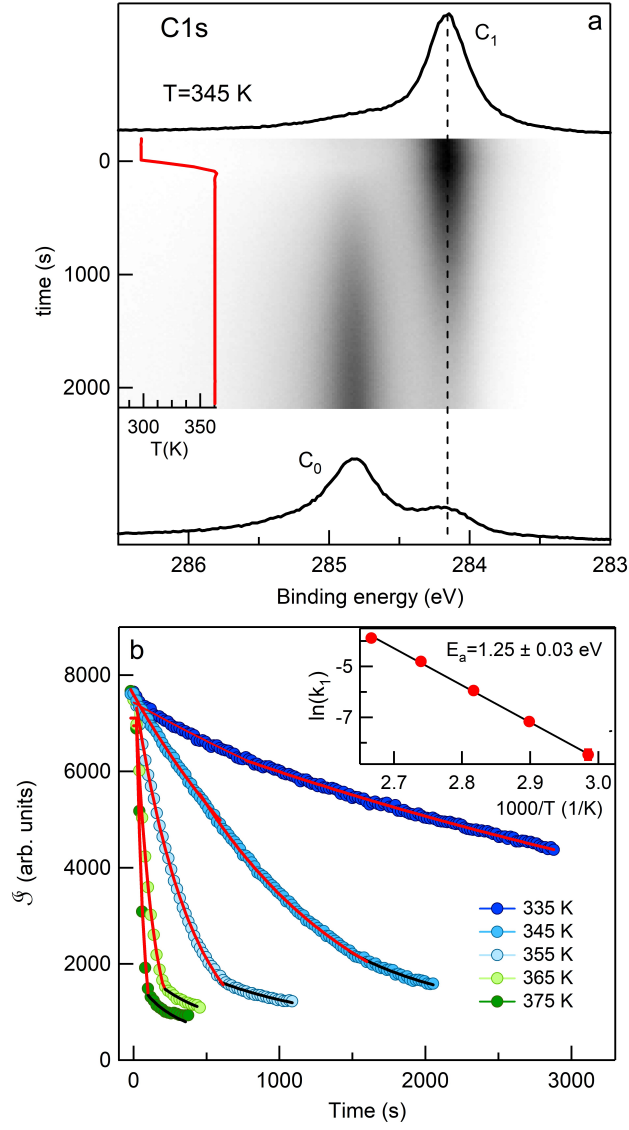


Figure 4: **Isothermal desorption from hydrogenated Gr/Ni(111).** (a) 2D plots of the C1s spectra measured during the hydrogen desorption at 345 K. The top and bottom C1s spectra were measured before and after (incomplete) hydrogen release, respectively. (b) Integrated intensity  $\mathcal{I}$  of the C1 component vs. time measured during the isothermal desorption at different temperatures of the Gr/Ni(111) sample hydrogenated at 289 K. The red and black lines superimposed onto the experimental data are the best-fit curves obtained for first- and second-order desorption process, respectively. The inset shows the Arrhenius plot of the rate constants  $k_1$  derived for the first-order desorption.



almost equivalent to those calculated without graphene (see Table 1). Then, the different yields of bulk absorption have to be related solely to the kinetics of the subsurface diffusion. Interestingly, a similar beneficial effect for the H storage due to the presence of Gr has not been observed for a strongly disordered Gr/Ni interface represented by a Ni foam covered by a single layer graphene.<sup>52</sup> In this case the defective graphene coating, which replicates the mosaicity of the Ni support is not effective in holding, more than the bare foam, the hydrogen diffused in the bulk and therefore in increasing significantly the stored amount with respect to the uncoated metal support.

In order to get more information about the desorption routes, we measured the deintercalation isotherms at selected temperature  $T_{des}$  in the range 335-375 K. For this experiment the hydrogen dose (30 klangmuir) was high enough to determine the almost complete decoupling of graphene from the substrate proved by the nearly total lack of the  $C_0$  component in the C1s spectrum (see the upper panel in Figure 4a). The 2D plot of the C1s spectra measured during the isothermal desorption at 345 K is displayed in the middle panel of Figure 4a, whereas the bottom panel shows the C1s spectrum measured after 2100 s. The integrated intensity  $\mathfrak{I}$  of the peak  $C_1$  measured as function of the time is reported for each desorption temperature in Figure 4b.  $H_2$  desorption after surface H-H recombination is a second order process. On the other hand, if the desorption of surface H atoms occurs via the recombination with H atoms emerging from the bulk and the process is fast, for each event graphene only feels the loss of the surface atom and the desorption revealed by the C1s spectra can be considered a first-order process. Using the Polanyi-Wigner relation to describe the desorption rate  $-d\theta_{Ni}/dt = k_\alpha \theta_{Ni}^\alpha$ , where  $\alpha=1, 2$  is the process order and  $k_\alpha$  is the corresponding rate constant, leads to  $\theta_{Ni}(t) = \theta_0 e^{-kt}$  for  $\alpha=1$  and to  $\theta_{Ni}(t) = \theta_0(1 + k\theta_0 t)^{-1}$  for  $\alpha=2$ ,  $\theta_0$  being the initial surface coverage. In our case  $\theta_{Ni}$  is proportional to  $\mathfrak{I}$ , as the coverage of intercalated H residing on the Ni(111) surface determines the intensity of the  $C_1$  peak in the C1s spectrum. Therefore,  $\ln \mathfrak{I}(t)$  for  $\alpha=1$  and  $1/\mathfrak{I}(t)$  for  $\alpha=2$  should show a linear trend as a function of  $t$ . The plots of  $\ln \mathfrak{I}(t)$  and  $1/\mathfrak{I}(t)$  vs  $t$  (see Figure S2) show complex

shapes, which demonstrate that the reaction order changes during the desorption depending on surface coverage and temperature. Our analysis leads to the conclusion that, at any investigated temperature, the desorption initiates as a first order process and that, when the surface coverage has strongly decreased, possibly switches to a second order process. The best-fit curves obtained according to a first-order (red lines) followed by a second-order (black lines) desorption are superimposed on the experimental data in Figure 4b. This behavior indicates that, during the extended first part of the desorption, graphene lands on the Ni substrate as if  $\theta_{Ni}$  is consumed following a first order process, which likely means that most of the surface H atoms recombine with H atoms migrating from the bulk. The desorption at 335 K represents an exception as the corresponding  $\mathfrak{I}(t)$  vs.  $t$  curve is entirely best-fitted as a first-order process, likely because at this temperature the probing time was too short to observe the transition to the other regime. The Arrhenius plot of the logarithm of the  $k_1$  rate constants vs. the inverse temperature shown in the inset of Figure 4b indicates an activation energy of 1.25 eV. It is worth considering that, as reported above, the calculated energy barrier for resurfacing on the Ni(111) surface at  $\theta_{Ni}$  of 1 monolayer is 0.65 eV,<sup>15</sup> a value slightly higher than the activation barriers between 0.5 and 0.6 eV<sup>7,15</sup> reported for associative desorption, for both H atoms which recombine staying in hollow sites of the Ni surface. The higher energy barrier we find has to be evaluated by considering that the presence of graphene undoubtedly represents an additional obstacle that the desorbing molecules must overcome to reach the free space and therefore is expected to alter the energetics for H<sub>2</sub> evolution with respect to the bare Ni(111) surface.

## Conclusions

In this study we have combined C1s spectroscopy and DFT calculations to deepen the knowledge on the surface and bulk processes occurring during the interaction of H atoms with the Gr/Ni(111) interface. Our experimental findings clearly illustrate the role that

the sample temperature plays in the delicate interplay between chemisorption on graphene and intercalation below graphene. The calculated energetics of the hydrogenated system optimally clarify the observed evolution of the interface configuration with the amount of dosed hydrogen. XPS and TPD results demonstrated that for Gr/Ni(111) it is possible, at RT, to saturate the Ni surface and to store in the bulk a certain amount of H, which depends on the delivered dose. Notably, without Gr, the H coverage at the Ni surface appears reduced and the amount diffused in the bulk results more than halved. As we have discussed above, because a high occupation at Ni surface sites decreases both the energy barrier for diffusion subsurface and the resurfacing rate through the so-called *capping effect*,<sup>7</sup> having the Ni surface fully hydrogenated facilitates H penetration in the bulk and inhibits resurfacing, strongly enhancing the efficiency of H storage. Hence, the key-role of the Gr cover: it makes it possible that the accumulated coverage at the Ni surface, protected from the incoming H-flux, becomes an efficient mean to convey the H atoms in the metal bulk and to stabilize them with respect to anticipated desorption. According to the analysis of the isothermal desorption curves, H<sub>2</sub> release is mostly triggered by the recombination between H atoms residing on the Ni surface with atoms migrating from the metal bulk. The demonstration that graphene can 'seal' to some extent a good sorption metal as nickel loaded with hydrogen, might have interesting implications for the design of novel materials and interfaces to be applied for H storage.

## Acknowledgement

R.L. acknowledges support from grant HPRIDE ("Production and storage of hydrogen in nanostructured graphene/nickel systems"; Grant 85-2017-15316), funded by LazioInnova/Regione Lazio in the frame "Progetti di Gruppi di Ricerca" (L.R. Lazio 13/08). "M.P. and D.A. are supported by the Natural Environment Research Council (Grant NE/R000425/1). This work used the ARCHER2 UK National Supercomputing Service (<https://www.archer2.ac.uk>). We acknowledge Elettra Sincrotrone Trieste for providing access to its synchrotron radiation facilities and for financial support.

Table 1: Adsorption Energy per H Atom  $E_a$  (in eV) Calculated for the Different Configurations of the Hydrogenated Ni(111) surface and Gr/Ni(111) Interface Reported in the Leftmost Column. For each configuration the adsorption energie values refer to the underlined H atom and are calculated as a function of coverage and/or adsorption site.

<u>H</u> /Ni(111)		monomer	0.25 ML	1 ML	2 ML
	H <sub>FCC</sub>	-3.13	-3.07	-3.07	-2.29
	H <sub>HCP</sub>	-3.12	-3.06	-3.01	
	H <sub>TOP</sub>	-2.56			
	H <sub>BRIDGE</sub>	-3.00			
<u>H</u> /Gr/Ni(111)			0.125 ML	0.25 ML	0.5 ML
	monomer <sub>FCC</sub>	-2.42			
	paradimer <sub>FCC</sub>	-2.42			
	trimer <sub>FCC</sub>	-2.41			
	tetramer <sub>FCC</sub>	-2.46			
	eptamer <sub>FCC</sub>	-2.38			
	decamer <sub>FCC</sub>	-2.34			
	monomer <sub>TOP</sub>	-1.83			
	H/C <sub>FCC</sub>		-2.41	-2.40	-2.27
	H/C <sub>TOP</sub>		-1.83	-1.94	-2.03
Gr/ <u>H</u> /Ni(111)		monomer	0.25 ML <sub>Ni</sub>	1 ML <sub>Ni</sub>	
	H <sub>FCC</sub>	-2.10	-2.70	-2.94	
	H <sub>HCP</sub>	-2.12	-2.70	-2.93	
	H <sub>TOP</sub>	-0.95			
	H <sub>BRIDGE1</sub>	-2.10			
	H <sub>BRIDGE2</sub>	-2.12			
<u>H<sub>FCC</sub></u> /Gr/1ML-H <sub>FCC</sub> /Ni(111)		monomer	eptamer	decamer	
		-2.83	-2.40	-2.37	
H(monomer) <sub>FCC</sub> /Gr/ <u>H<sub>FCC</sub></u> /Ni(111)		monomer	0.25 ML <sub>Ni</sub>	1 ML <sub>Ni</sub>	
		-2.35	-2.40	-2.83	
1ML-H <sub>FCC</sub> /Ni(111)/ <u>H</u>		monomer <sub>oct</sub>	monomer <sub>tetra</sub>	1 ML <sub>tetra</sub>	
		-2.98	-2.97	-2.70	
Gr/1ML-H <sub>FCC</sub> /Ni(111)/ <u>H</u>		monomer <sub>oct</sub>	monomer <sub>tetra</sub>	1 ML <sub>tetra</sub>	
		-2.93	-2.92	-2.67	

## Supporting Information Available

The Supporting Information is available free of charge.

- Analysis of the C1s spectra measured for Gr/Ni(111) hydrogenated at different temperatures; analysis of the isothermal desorption curves measured for the hydrogenated Gr/Ni(111); stability of the graphene coverage during Gr/Ni(111) hydrogenation (PDF).

## References

- (1) Hofman, M. S.; Wang, D. Z.; Yang, Y.; Koel, B. E. Interactions of incident H atoms with metal surfaces. *Surf. Sci. Rep.* **2018**, *73*, 153–189.
- (2) Bünermann, O.; Kandratsenka, A.; Wodtke, A. M. Inelastic scattering of H atoms from surfaces. *J. Phys. Chem. A* **2021**, *125*, 3059–3076.
- (3) Karst, J.; Sterl, F.; Linnenbank, H.; Weiss, T.; Hentschel, M.; Giessen, H. Watching in situ the hydrogen diffusion dynamics in magnesium on the nanoscale. *Sci. Adv.* **2020**, *6*, eaaz0566.
- (4) Christmann, K.; Schober, O.; Ertl, G.; Neumann, M. Adsorption of hydrogen on nickel single crystal surfaces. *J. Chem. Phys.* **1974**, *60*, 4528–4540.
- (5) Cao, G. X.; Nabighian, E.; Zhu, X. D. Diffusion of hydrogen on Ni(111) over a wide range of temperature: exploring quantum diffusion on metals. *Phys. Rev. Lett.* **1997**, *79*, 3696–3699.
- (6) Premm, H.; Pölzl, H.; Winkler, A. Dynamics and kinetics of subsurface absorption and desorption for the system hydrogen (deuterium)–Ni(111). *Surf. Sci.* **1998**, *401*, L444–L451.
- (7) Baer, R.; Zeiri, Y.; Kosloff, R. Hydrogen transport in nickel (111). *Phys. Rev. B* **1997**, *55*, 10952–10974.

- (8) Michaelides, A.; Hu, P.; Alavi, A. Physical origin of the high reactivity of subsurface hydrogen in catalytic hydrogenation. *J. Chem. Phys.* **1999**, *111*, 1343–1345.
- (9) Ledentu, V.; Dong, W.; Sautet, P. Heterogeneous catalysis through subsurface sites. *J. Amer. Chem. Soc.* **2000**, *122*, 1796–1801.
- (10) Ceyer, S. T. The unique chemistry of hydrogen beneath the surface: catalytic hydrogenation of hydrocarbons. *Acc. Chem. Res.* **2001**, *34*, 737–744.
- (11) Sha, X.; Jackson, B. Ab initio and transition state theory studies of the energetics of H atom resurfacing on Ni(1 1 1). *Chem. Phys. Lett.* **2002**, *357*, 389–396.
- (12) Wright, S.; Skelly, J. F.; Hodgson, A. Energy disposal during desorption of D<sub>2</sub> from the surface and subsurface region of Ni(111). *Faraday Discuss.* **2000**, *117*, 133–146.
- (13) Greeley, J.; Krekelberg, W. P.; Mavrikakis, M. Strain-induced formation of subsurface species in transition metals. *Ang. Chemie Int. Ed.* **2004**, *43*, 4296–4300.
- (14) Bhatia, B.; Sholl, D. S. Chemisorption and diffusion of hydrogen on surface and subsurface sites of flat and stepped nickel surfaces. *J. Chem. Phys.* **2005**, *122*, 204707.
- (15) Shirazi, M.; Bogaerts, A.; Neyts, E. C. A DFT study of H-dissolution into the bulk of a crystalline Ni(111) surface: a chemical identifier for the reaction kinetics. *Phys. Chem. Chem. Phys.* **2017**, *19*, 19150–19158.
- (16) Traisnel, C.; Metsue, A.; Oudriss, A.; Bouhattate, J.; Feaugas, X. Hydrogen solubility and diffusivity near surface of nickel single crystals: some implications of elastic energy. *Comput. Mat. Sci.* **2021**, *188*, 110136.
- (17) Wang, W.; He, Y. H Resurface and hot H promoted H<sub>2</sub> recombination on Ni(111): effects of arrangement, surface coverage, and lattice motion. *J. Phys. Chem. C* **2021**, *125*, 6650–6659.

- (18) Hopkinson, A. R.; Probert, M. I. J. Quantum diffusion of H/D on Ni(111)—A partially adiabatic centroid MD study. *J. Chem. Phys.* **2018**, *148*, 102339.
- (19) Torres, E.; Pencer, J.; Radford, D. Atomistic simulation study of the hydrogen diffusion in nickel. *Comput. Mat. Sci.* **2018**, *152*, 374–380.
- (20) Zhao, W.; Gebhardt, J.; Späth, F.; Gotterbarm, K.; Gleichweit, C.; Steinrück, H.-P.; Görling, A.; Papp, C. Reversible hydrogenation of graphene on Ni(111)—synthesis of ‘graphone’. *Chem. Eur. J.* **2015**, *21*, 3347–3358.
- (21) Soni, H. R.; Gebhardt, J.; Görling, A. The reactivity of substrate-supported graphene: a case study of hydrogenation. *J. Phys. Chem. C* **2018**, *122*, 2761–2772.
- (22) Zhang, L.; Jia, Y.; Gao, G.; Yan, X.; Chen, N.; Chen, J.; Soo, M. T.; Wood, B.; Yang, D.; et al., A. D. Graphene defects trap atomic Ni species for hydrogen and oxygen evolution reactions. *Chem* **2018**, *4*, 285–297.
- (23) Lizzit, D.; Trioni, M. I.; Bignardi, L.; Lacovig, P.; Lizzit, S.; Martinazzo, R.; Larciprete, R. Dual-route hydrogenation of the graphene/Ni interface. *ACS Nano* **2019**, *13*, 1828–1838.
- (24) Feulner, P.; Menzel, D. Simple ways to improve flash desorption measurements from single crystal surfaces. *J. Vac. Sci. Technol.* **1980**, *17*, 662–663.
- (25) Kresse, G.; Furthmüller, J. Efficient iterative schemes for ab initio total-energy calculations using a plane-wave basis set. *Phys. Rev. B* **1996**, *54*, 11169–11186.
- (26) Hamada, I. van der Waals density functional made accurate. *Phys. Rev. B* **2014**, *89*, 121103.
- (27) Blöchl, P. E. Projector augmented-wave method. *Phys. Rev. B* **1994**, *50*, 17953–17979.
- (28) Perdew, J. P.; Burke, K.; Ernzerhof, M. Generalized gradient approximation made simple. *Phys. Rev. Lett.* **1996**, *77*, 3865–3868.



- (29) Henkelman, G.; Uberuaga, B. P.; Jónsson, H. A climbing image nudged elastic band method for finding saddle points and minimum energy paths. *J. Chem. Phys.* **2000**, *113*, 9901–9904.
- (30) Andersen, M.; Hornekaer, L.; Hammer, B. Graphene on metal surfaces and its hydrogen adsorption: a meta-GGA functional study. *Phys. Rev. B* **2012**, *86*, 085405.
- (31) Harris, J.; Kasemo, B. On precursor mechanisms for surface reactions. *Surf. Sci.* **1981**, *105*, L281–L287.
- (32) Strömquist, J.; Bengtsson, L.; Persson, M.; Hammer, B. The dynamics of H absorption in and adsorption on Cu(111). *Surf. Sci.* **1998**, *397*, 382–394.
- (33) Shalashilin, D. V.; Jackson, B. Formation and dynamics of hot-precursor hydrogen atoms on metal surfaces: Trajectory simulations and stochastic models. *J. Chem. Phys.* **1998**, *109*, 2856–2864.
- (34) Shikin, A. M.; Farías, D.; Rieder, K. H. Phonon stiffening induced by copper intercalation in monolayer graphite on Ni(111). *Europhys. Lett.* **1998**, *44*, 44–49.
- (35) Shikin, A.; Farías, D.; Adamchuk, V.; Rieder, K.-H. Surface phonon dispersion of a graphite monolayer adsorbed on Ni(111) and its modification caused by intercalation of Yb, La and Cu layers. *Surf. Sci.* **1999**, *424*, 155–167.
- (36) Sun, P. Z.; Yang, Q.; Kuang, W. J.; Stebunov, Y. V.; Xiong, W. Q.; Yu, J.; Nair, R. R.; Katsnelson, M. I.; Yuan, S. J.; Grigorieva, e. a. Limits on gas impermeability of graphene. *Nature* **2020**, *579*, 229–232.
- (37) Bartolomei, M.; Hernández, M. I.; Campos-Martínez, J.; Hernández-Lamonedá, R.; Giorgi, G. Permeation of chemisorbed hydrogen through graphene: A flipping mechanism elucidated. *Carbon* **2021**, *178*, 718–727.

- (38) Balog, R.; Andersen, M.; Jørgensen, B.; Sljivancanin, Z.; Hammer, B.; Baraldi, A.; Larciprete, R.; Hofmann, P.; Hornekær, L.; Lizzit, S. Controlling hydrogenation of graphene on Ir(111). *ACS Nano* **2013**, *7*, 3823–3832.
- (39) Zhou, Y.; Chen, W.; Cui, P.; Zeng, J.; Lin, Z.; Kaxiras, E.; Zhang, Z. Enhancing the hydrogen activation reactivity of nonprecious metal substrates via confined catalysis underneath graphene. *Nano Lett.* **2016**, *16*, 6058–6063.
- (40) Bhatia, B.; Sholl, D. S. Chemisorption and diffusion of hydrogen on surface and sub-surface sites of flat and stepped nickel surfaces. *J. Chem. Phys.* **2005**, *122*, 204707.
- (41) Greeley, J.; Mavrikakis, M. A first-principles study of surface and subsurface H on and in Ni(111): diffusional properties and coverage-dependent behavior. *Surf. Sci.* **2003**, *540*, 215–229.
- (42) Johnson, A. D.; Maynard, K. J.; Daley, S. P.; Yang, Q. Y.; Ceyer, S. T. Hydrogen embedded in Ni: production by incident atomic hydrogen and detection by high-resolution electron energy loss. *Phys. Rev. Lett.* **1991**, *67*, 927–930.
- (43) Wang, W.; Zhao, Y. Quantum instanton evaluations of surface diffusion, interior migration, and surface-subsurface transport for H/Ni. *J. Chem. Phys.* **2010**, *132*, 064502.
- (44) Eberhardt, W.; Greuter, F.; Plummer, E. W. Bonding of H to Ni, Pd, and Pt Surfaces. *Phys. Rev. Lett.* **1981**, *46*, 1085–1088.
- (45) Pétuya, R.; Larrégaray, P.; Crespos, C.; Aurel, P.; Busnengo, H. F.; Martínez, A. E. Scattering of Atomic Hydrogen Off a H-Covered W(110) Surface: Hot-Atom versus Eley-Rideal Abstraction Dynamics. *J. Phys. Chem. C* **2015**, *119*, 3171–3179.
- (46) Gdowski, G.; Felter, T.; Stulen, R. Effect of surface temperature on the sorption of hydrogen by Pd(111). *Surf. Sci. Lett.* **1987**, *181*, L147–L155.

- (47) Castro, F. J.; Sánchez, A. D.; Meyer, G. Bulk effects in thermal desorption spectroscopy. *J. Chem. Phys.* **1998**, *109*, 6940–6946.
- (48) Kammler, T.; Wehner, S.; Küpper, J. Interaction of thermal H atoms with Ni(100)-H surfaces: through surface penetration and adsorbed hydrogen abstraction. *Surf. Sci.* **1995**, *339*, 125–134.
- (49) Mavrikakis, M.; Schwank, J. W.; Gland, J. L. The effects of exposure time and pressure on the temperature-programmed desorption spectra of systems with bulk states. *Surf. Sci.* **1996**, *355*, L385–L392.
- (50) Behm, R. J.; Penka, V.; Cattania, M.; Christmann, K.; Ertl, G. Evidence for 'sub-surface' hydrogen on Pd(110): An intermediate between chemisorbed and dissolved species. *J. Chem. Phys.* **1983**, *78*, 7486–7490.
- (51) Mudiyanse, K.; Yang, Y.; Hoffmann, F. M.; Furlong, O. J.; Hrbek, J.; White, M. G.; Liu, P.; Stacchiola, D. J. Adsorption of hydrogen on the surface and sub-surface of Cu(111). *J. Chem. Phys.* **2013**, *139*, 044712.
- (52) Petrone, G.; Zarotti, F.; Lacovig, P.; Lizzit, D.; Tosi, E.; Felici, R.; Lizzit, S.; Larciprete, R. The effect of structural disorder on the hydrogen loading into the graphene/nickel interface. *Carbon* **2022**, *199*, 357–366.

# TOC Graphic

